ELSEVIER

Journal of Photochemistry and Photobiology A: Chemistry 151 (2002) 57–65

Journal of Photochemistry and Photobiology A:Chemistry

www.elsevier.com/locate/jphotochem

Photophysical behavior of molecular dyads and triad comprising tris(bipyrazine)ruthenium^{II}, bis(bipyridine)chlororuthenium^{II} and pentacyanoferrate^{II} complexes

Sheila G. Camera, Henrique E. Toma*

Instituto de Química, Universidade de São Paulo, Caixa Postal 26077, CEP 05513-970, São Paulo, SP, Brazil

Received 5 November 2001; received in revised form 14 March 2002; accepted 26 March 2002

Abstract

We report three new systems containing tris(bipyrazine)ruthenium^{II} attached to bis(bipyridine)chlororuthenium$^{II/III}$ and/or pentacyanoferrate$^{II/III}$ complexes via the bipyrazine (bpz) bridging ligand, i.e. $[Ru(bpz)_3Ru(bipy)_2Cl]^{3+/4+}$, $[Ru(bpz)_3Fe(CN)_5]^{-/0}$ and $[(CN)_5Fe^{III}(bpz)Ru^{II}(bpz)_2Ru^{II}(bipy)_2Cl]^{+}$, (bipy: 2,2′-bipyridine). The excitation at 440 nm of the $[Ru^{II}(bpz)_3Ru^{II}(bipy)_2Cl]^{3+}$ complex leads to a ^{1}MLCT state which undergoes efficient intersystem crossing to the corresponding ^{3}MLCT state, $[Ru^{III}(bpz^-)_3Ru^{II}(bipy)_2Cl]^{3+}$. The conversion to the inverted mixed valence state, $[Ru^{II}(bpz^-)_3Ru^{III}(bipy)_2Cl]^{3+}$, proceeds via electron transfer mechanisms, competing with the radiative and nonradiative decay of the ^{3}MLCT state. A similar behavior was observed for the $[Ru^{II}(bpz)_3Fe^{II}(CN)_5]^-$ complex. In the case of the $[(CN)_5Fe^{III}(bpz)Ru^{II}(bpz)_2Ru^{II}(bipy)_2Cl]^-$ triad, the excited state centered on the $[Ru(bpz)_3]^{2+}$ moiety can undergo intramolecular electron transfer with the peripheral Ru^{II} and Fe^{III} groups, promoting effective charge-separation in the inverted mixed valence complex, $[(CN)_5Fe^{II}(bpz)Ru^{II}(bpz)_2Ru^{III}(bipy)_2Cl]^{+}$.
© 2002 Elsevier Science B.V. All rights reserved.

Keywords: Supramolecular photochemistry; Photoinduced electron transfer; Ruthenium complexes; Iron complexes; Photochemical charge-separation

1. Introduction

Polynuclear metal complexes containing phophysically active centers are particularly interesting from the point of view of photoinduced electron transfer and energy transfer processes [1–5]. The presence of a metal complex attached to the photoactive center via a bridging ligand provides additional pathways for the deactivation of the excited states, and in some cases can promote effective charge-separation, giving rise to molecular dyad and triad devices. In these systems, the geometry, intermetallic separation distance, and electronic properties of the bridging ligands are relevant factors to be considered, in addition to the photochemical and photophysical characteristics of the metal ions.

The assembly of dyads and triads based on the photoactive, multibridging tris(bipyrazine)ruthenium^{II} complex directly bound to transition metal complexes, has never been reported before. However, this strategy, which follows a coordination chemistry approach, has been previously employed in the design of symmetric supermolecules, such as the heptanuclear complexes derived from $[Ru(bpz)_3]^{2+}$ [6–9] (bpz: bipyrazine). Now, we report two new systems containing a tris(bipyrazine)ruthenium^{II} ion attached to bis(bipyridine) chlororuthenium$^{II/III}$ or pentacyanoferrate$^{II/III}$ complexes via a bipyrazine bridging ligand, e.g. $[Ru(bpz)_3Ru(bipy)_2Cl]^{3+/4+}$ or $[Ru(bpz)_3Fe(CN)_5]^{-/0}$, as shown in Fig. 1A, B (bipy: 2,2′-bipyridine). For simplicity, the ruthenium ions in the $[Ru(bpz)_3]^{2+}$ and $[Ru(bipy)_2Cl]^{+}$ moieties will be denoted Ru_c and Ru_p, respectively. These binuclear complexes can behave as photochemical dyads, exhibiting photoinduced electron transfer between the two metal centers. In addition, by attaching both complexes to the $[Ru(bpz)_3]^{2+}$ center, the triad system $[(CN)_5Fe^{III}(bpz)_2Ru^{II}(bpz)Ru^{II}(bipy)_2Cl]^{+}$ (Fig. 1C) can be obtained, after suitable oxidation of the iron^{II} sites. In this case, a long distance charge-separation is expected from photoinduced electron-transfer processes within the trinuclear complex, generating the inverted mixed-valence $[Fe^{II}(bpz)Ru^{II}_c(bpz)Ru^{III}_p]$ species (Fig 1C).

* Corresponding author. Tel.: +55-11-3818-3887; fax: +55-11-3815-5579.
E-mail address: henetoma@iq.usp.br (H.E. Toma).

1010-6030/02/$ – see front matter © 2002 Elsevier Science B.V. All rights reserved.
PII: S1010-6030(02)00150-8

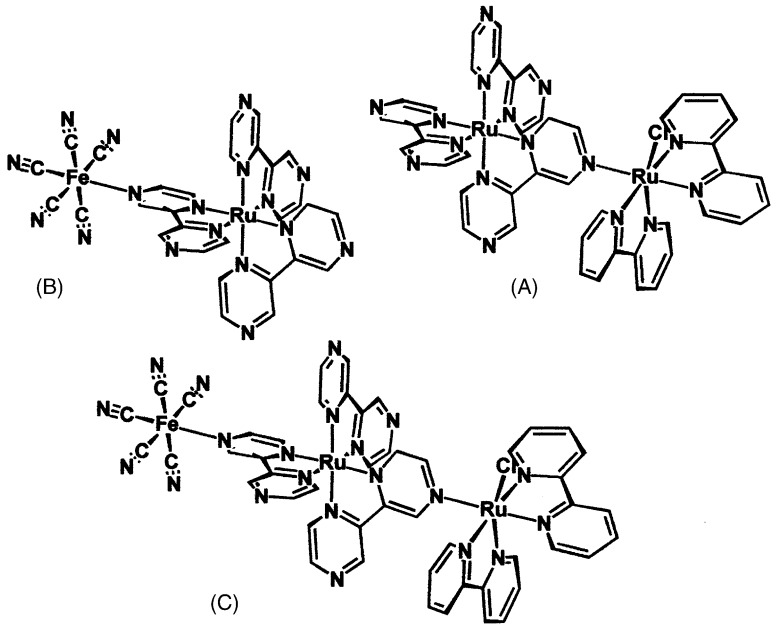

Fig. 1. Structural representations of the $[Ru(bpz)_3Ru(bipy)_2Cl]^{3+}$ (A), $[Ru(bpz)_3Fe(CN)_5]^{-}$ (B) and $[(CN)_5Fe^{III}(bpz)_2Ru^{II}(bpz)Ru^{II}(bipy)_2Cl]^{+}$ (C) systems.

2. Experimental section

2.1. Synthesis

The $[Ru(bpz)_3]Cl_2{\cdot}3.5H_2O$ [10–12], *cis*-$[Ru(bpy)_2Cl_2]{\cdot}2H_2O$ [13] and $Na_3[Fe(CN)_5NH_3]{\cdot}3H_2O$ [14] complexes were prepared as described in the literature. $[Ru(bpy)_2(pz)Cl]PF_6{\cdot}H_2O$ was prepared by refluxing 0.30 g of *cis*-$[Ru(bpy)_2Cl_2]{\cdot}2H_2O$ (0.57 mmol) and 0.54 g (6.8 mmol) of pyrazine (pz), dissolved in 80 cm^3 of *N*,*N*′-dimethylformamide, during 4 h. The solvent was removed using a rotary evaporator, and the solid residue was dissolved in 7 cm^3 of ethanol. After adding 0.48 g of NH_4PF_6 (2.9 mmol) dissolved in 2 cm^3 ethanol:water (1:1), the mixture was kept in the freezer. The solid was collected on a filter, washed with 10 cm^3 of water and dried under vacuum in the presence of calcium chloride. Anal. calcd for $RuC_{24}N_6H_{22}OClPF_6$: C, 41.7; H, 3.2; N, 12.2. Found: C, 42.1; H, 3.7; N, 11.9%.

The bimetallic $[Ru^{II}(bpz)_3Ru^{II}(bpy)_2Cl](PF_6)_3{\cdot}3.5H_2O$ complex was synthesized by reacting under reflux, 0.063 g of $[Ru(bpz)_3]Cl_2{\cdot}3.5H_2O$ (0.89 mmol) with 0.049 g of *cis*-$[Ru(bpy)_2Cl_2]{\cdot}2H_2O$ (0.98 mmol) in 40 cm^3 of ethanol:water (1:3). After 80 min, 0.0095 g of lithium chloride (0.22 mmol) was added, and the reflux was maintained for 20 min. The solution was concentrated almost to dryness in a rotary evaporator, and diluted with 20 cm^3 of ethanol. Then, 0.25 g of NH_4PF_6 (1.5 mmol) dissolved in 2 cm^3 of water was added, and the solution was kept overnight in the freezer. The solid product was collected on a filter and washed with 5 cm^3 of cold water. Purification was carried out by Al_2O_3 column chromatography, by dissolving into a minimum volume of acetonitrile and eluting with 1:4 methanol:acetonitrile solution. Finally, the solid residue obtained after evaporation, was dissolved into a minimum volume of acetonitrile, and precipitated by adding diethyl ether. The pure compound was colleted on a filter, and dried under vacuum. Anal. calcd for $C_{44}H_{41}N_{16}O_{3.5}ClRu_2P_3F_{18}$: C, 34.7; H, 2.7; N, 14.7. Found: C, 34.2; H, 3.0; N, 14.5.

The $[Ru(bpz)_3Fe(CN)_5]^{-}$ and $[(CN)_5Fe^{III}(bpz)_2Ru^{II}(bpz)Ru^{II}(bipy)_2Cl]^{+}$ complexes were generated in aqueous solution, by the direct reaction of the $[Ru(bpz)_3]^{2+}$ or $[Ru^{II}(bpz)_3Ru^{II}(bpy)_2Cl]^{+}$ complexes with $[Fe(CN)_5NH_3]^{3-}$ under (1:1) stoichiometric conditions. It should be noticed that the binding of the pentacyanoferrate^{II} complexes to the tris(bipyrazine)ruthenium^{II} complexes proceeds in a quantitative way ($K > 10^7\ M^{-1}$), and under stoichiometric conditions the formation of 2:1 and higher complexes is precluded from the selective charge-effects involved in the kinetics [6].

2.2. Physical measurements

All the electrochemical and optical measurements were carried out under an argon atmosphere. Cyclic voltammetry measurements were carried out using a Princeton Applied Research model 173 potentiostat and a model 175 universal programmer, as described previously [9]. All potentials are referred to the standard hydrogen electrode (SHE). The electronic spectra were recorded on a Guided Wave model 260 fiber optics spectrophotometer, or on a Hewlett Packard 8453-A diode-array equipment. Fluorescence

measurements were carried out on a Photon Technology (PTI) model LS-100 instrument, equipped with near-IR-sensitive photomultipliers. The luminescence spectra in ethanol glass at 77 K were obtained using a low-temperature accessory from PTI and a quartz cell. In situ absorption spectroelectrochemical measurements were carried out using the Guided Wave fiber optics bundle probe directed to the surface of the mirror platinum working electrode, which was positioned parallel to the flat bottom of the electrochemical quartz cell in order to provide an adjustable thin layer arrangement. Lifetime measurements were carried out using the PTI instrument and the corresponding software package for kinetic analysis, or by means of flash photolysis, using an Edinburgh Analytical Instruments model LP900S1 system consisting of a continuum Surelite II-10 laser (λ_{exc} = 355 nm), a XP900 monitoring xenon lamp, a monocromator, photomultiplier and a Tectronics oscilloscope.

2.3. Molecular calculations

Semiempirical molecular orbital calculations for the $[Ru^{II}(bpz)_3Ru^{II}(bpy)_2Cl]^{3+}$ complex were carried out using the ZINDO/S method, after molecular mechanics geometry optimizations using the MM+ module from HyperChem 6.1, as detailed in our previous publications on related ruthenium^{II}-polyimine complexes [15–18].

3. Results and discussion

3.1. Photophysical behavior of the diad $[Ru^{II}(bpz)_3Ru^{II}(bipy)_2Cl]^{3+}$

The $[Ru^{II}(bpz)_3Ru^{II}(bpy)_2Cl]^{3+}$ complex comprises a tris(bipyrazine)ruthenium^{II} center bound to the $Ru^{II}(bpy)_2Cl^{+}$ moiety via the peripheral nitrogen atom of the bridging bipyrazine ligand, as shown in Fig. 1. For discussion purposes, the electronic properties of this bimetallic complex will be compared with those of the related chromophore species, $[Ru(bpz)_3]^{2+}$ [10–13] and *cis*-$[Ru(bpy)_2Cl(pz)]^{+}$ (pz: pyrazine).

Typical cyclic voltammograms for the bimetallic complex are shown in Fig. 2. The reversible wave at $E_{1/2}$ = 1.14 V versus SHE can be ascribed to the $Ru_p^{III/II}$ redox couple. The measurement of E^0 for the $[Ru(bpz)_3]^{3+/2+}$ couple was precluded by the solvent working range, and the previously reported value of 2.08 V [10–13] for the mononuclear species, was assumed in this work. Three successive, nearly reversible waves, corresponding to the reduction of the bipyrazine ligands, can be observed at $E_{1/2}$ −0.37, −0.63 and −0.84 V (Fig. 2), in comparison with −0.44, −0.63 and −0.90 V, for the $[Ru(bpz)_3]^{2+}$ complex [10–13]. The reduction of the bipyridine ligands in the *cis*-$[Ru(bipy)_2Cl]^{+}$ moiety is expected to occur below −1 V, and may be responsible for the shoulder at −1.30 V (Fig. 2).

The electronic spectrum of the $[Ru(bpz)_3]^{2+}$ complex is characterized by two strong bands at 443 and 342 nm, ascribed to $d_\pi \rightarrow \pi_1^*, \pi_2^*$ metal-to-ligand charge-transfer (MLCT) transitions [10]. The electronic spectrum of the *cis*-$[Ru(bpy)_2Cl(pz)]^{2+}$ complex exhibits two sets of composite bands, at 489 ($\varepsilon = 6.6 \times 10^3\,M^{-1}\,cm^{-1}$), 446 ($4.5 \times 10^3$) nm and at 384 ($5.6 \times 10^3$), 337 ($4.7 \times 10^3$) nm, ascribed to $Ru^{II} \rightarrow \pi_1^*$(bipy) and $\pi_2{}^*$(bipy) charge-transfer transitions, respectively, and a weak shoulder at 565 (1.5×10^3) nm, ascribed to a $Ru^{II} \rightarrow \pi^*$(pz) charge-transfer transition.

The electronic spectrum of the bimetallic complex in the visible region (Figs. 2 and 3) exhibits two strong, composite bands at 575 and 440 nm. The relevant energy levels for this complex, based on the ZINDO/S method, are listed in Table 1, including the fractional orbital mixing. The electronic transitions can be reasonably simulated, as shown in Table 2.

According to the calculations, the electronic band at 575 nm arises from the excitation from MO 155 (HOMO), mainly localized on the $[Ru^{II}(bipy)_2Cl]^{+}$ moiety (71%, see Tables 1 and 2), to MO 156 (LUMO), mainly localized on the bridging bpz ligand (61%); thus, corresponding to

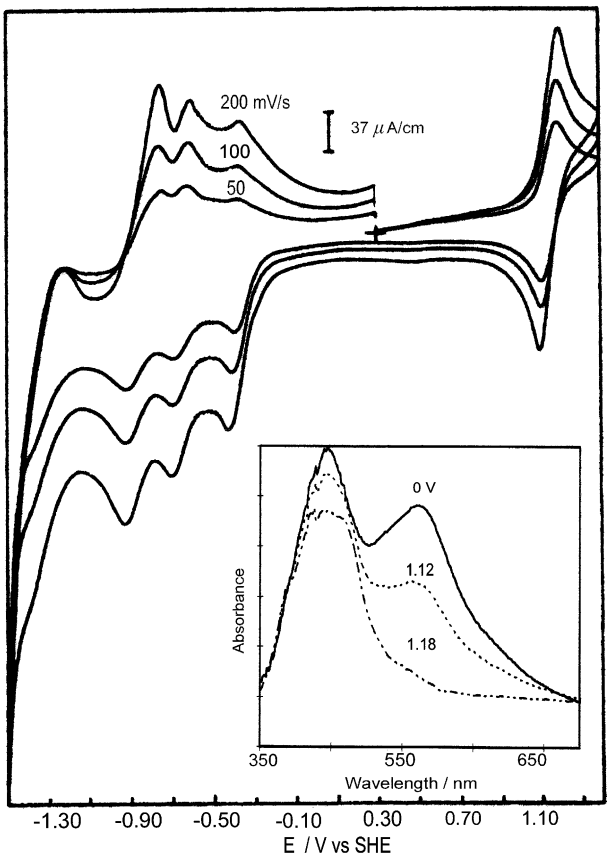

Fig. 2. Cyclic voltammograms of the $[Ru^{II}(bpz)_3Ru^{II}(bipy)_2Cl]^{3+}$ complex, at several scan rates, in acetonitrile solution (0.1 M tetraethylammonium perchlorate). Inset: spectroelectrochemical changes at 0, 1.12 and 1.18 V, accompanying the oxidation of the Ru_p^{II} moiety.

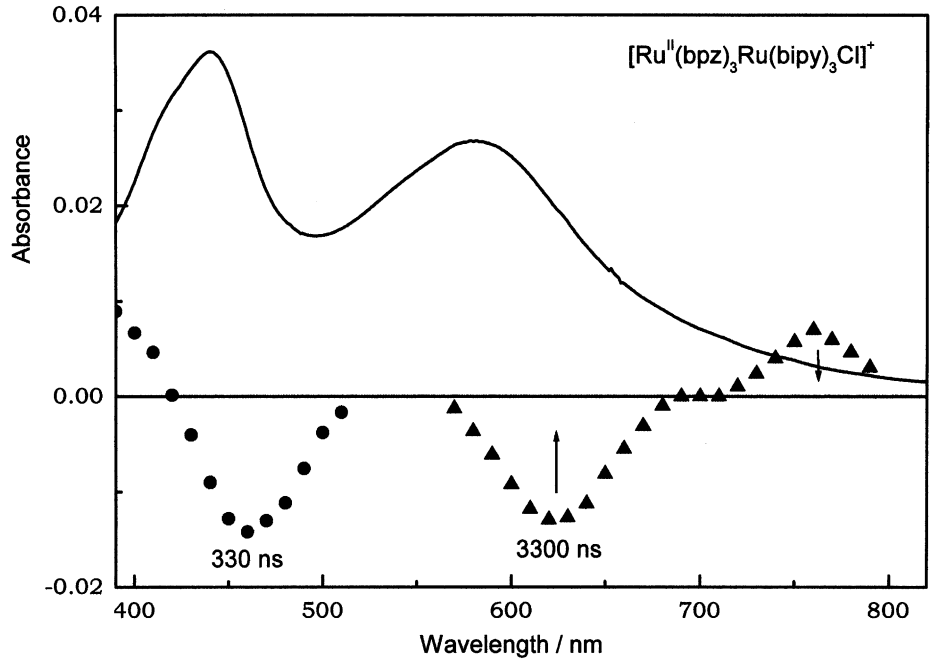

Fig. 3. Absorption profile (top, ×0.1) of the $[Ru^{II}(bpz)_3Ru^{II}(bipy)_2Cl]^{3+}$ complex (15 μM), in aqueous solution, showing the MLCT bands of the $[Ru^{II}(bpz)_3]^{2+}$ and $[(bpz)Ru(bipy)Cl]^{+}$ chomophores at 440 and 570 nm, respectively, and (bottom) time resolved differential spectra recorded at 330 and 3300 ns after laser pulse excitation.

Table 1
MO energy order and fractional orbital mixing of $[Ru_c^{II}(bpz)_3Ru_p^{II}(bipy)_2Cl]^{3+}$

MO number	Energy (eV)	Ru_c^{II}	Non-bridging bpz	Bridging bpz	Ru_p^{II}	bipy	Cl^-
149	−15.238	0.572	0.158	0.189	0.040	0.038	0.003
150	−15.196	0.007	0.002	0.002	0.014	0.975	0
151	−15.057	0.726	0.185	0.087	0.001	0.001	0
152	−15.031	0.650	0.287	0.058	0	0	0.005
153	−14.053	0.002	0.002	0.002	0.769	0.194	0.031
154	−13.973	0.010	0.003	0.030	0.758	0.177	0.016
155 (HOMO)	−13.196	0.081	0.029	0.182	0.517	0.190	0.001
156 (LUMO)	−8.975	0.021	0.237	0.608	0.071	0.063	0
157	−8.531	0.085	0.710	0.159	0.015	0.031	0
158	−8.359	0.113	0.841	0.043	0.001	0.001	0.001
159	−8.149	0.034	0.046	0.824	0.012	0.084	0
160	−7.761	0.014	0.974	0.012	0	0	0
161	−7.686	0.017	0.954	0.025	0	0.002	0.002
162	−7.553	0.002	0.008	0.130	0.090	0.770	0

Table 2
Main electronic transitions of $[Ru_c^{II}(bpz)_3Ru_p^{II}(bipy)_2Cl]^{3+}$ [a]

Experimental		Calculated (ZINDO/S)		Assignment, $Mo_i \rightarrow Mo_f$
λ (nm)	ε (M^{-1} cm^{-1})	λ (nm)	Osc. strength	
575	8.5×10^3	592	0.72	155 → 156 Ru_p → bpz (bridge)
Masked		487	0.15	155 → 159 Ru_p → bpz (bridge)
440	1.12×10^4	432	0.25	152 → 157 Ru_c → bpz (non-bridging)
410	Shoulder	400	0.15	149 → 156 Ru_c → bpz (bridge)

[a] Transitions exhibiting oscillator strengths >0.05, in the visible region.

a $Ru_p^{II} \rightarrow$ bpz (bridge) charge-transfer transition. Another related transition, from MO 155 to 159 (the last one exhibiting 82% bpz bridge character), is theoretically expected at 487 nm. It is, however, much less intense, being masked by the strong band at 575 nm. The second characteristic band, at 440 nm corresponds to the MO 152 → 157 transition centered on the $[Ru^{II}(bpz)_3]^{2+}$ chromophore. It is interesting to note that MO 152 involves 65% Ru_c^{II} + 29% non-bridging bpz character. There is only little contribution of the bridging bpz ligand (5.8%) to this level. Surprisingly, MO 157 exhibits 71% non-bridging bpz character, as compared with 16% for the bridging bpz one. Therefore, the absorption band at 440 nm involves preferential excitation of the Ru_c^{II} d_π electrons to the non-bridging bpz π^* levels, rather than to the bridging bpz ones. The high energy transition as a shoulder at 410 nm, corresponds to the MO 149 → 156 excitation, where the first MO has 57% Ru_c^{II} character and the second one, 61% bridging bpz character. These results indicate that in the $[Ru^{II}(bpz)_3]^{2+}$ moiety, the excitation to the bridging bpz π^* levels involves higher energies, as compared with the excitation to the corresponding non-bridging ligands.

The oxidation of the peripheral $[Ru(bipy)_2Cl]^+$ group was also monitored spectroelectrochemically, as shown in Fig. 2 (inset). Formation of the mixed valence Ru_c^{II}-bpz-Ru_p^{III} species, at 1.2 V, leads to the complete decay of the strong absorption band at 575 nm associated with the Ru_p^{II} species, with small changes in absorption profile of the $[Ru(bpz)_3]^{2+}$ group, around 440 nm. No evidence for intervalence transfer bands with $\varepsilon > 100\,dm^3\,mol^{-1}\,cm^{-1}$ has been detected in the visible and near-infrared region <1400 nm, indicating a weak electronic coupling between the Ru_c^{II} and Ru_p^{III} ions.

At 77 K, the bimetallic complex exhibits a characteristic emission band at 571 nm, and vibronic components at 620 and 670 nm. The emission, as monitored with the PTI instrument, was consistent with a single exponential decay, with a lifetime of 9.4 μs. The excitation spectrum exhibits a maximum at 450 nm, coinciding with the absorption band of the $[Ru(bpz)_3]^{2+}$ center. It is interesting to note that the parent $[Ru(bipy)_2(pz)Cl]^{2+}$ complex exhibits an emission band at 660 nm, with a shoulder at 696 nm. The corresponding excitation profile coincides with the absorption spectrum in the visible region. The measured lifetime in this case, at 77 K, was 6.1 μs. By comparing the emission and excitation spectra of the bimetallic $[Ru^{II}(bpz)_3Ru^{II}(bipy)_2Cl]^{3+}$ and the $[Ru(bipy)_2(pz)Cl]^{2+}$ complexes, one can infer that in the first case the emission takes place from the triplet MLCT level of $[Ru(bpz)_3]^{2+}$ moiety, rather than from the $[Ru(bipy)_2Cl]^+$ group.

At room temperature, the bimetallic complex exhibits only a weak asymmetric emission band at 608 nm, associated with the $[Ru(bpz)_3]^{2+}$ center, indicating substantial quenching from the $[Ru(bipy)_2Cl]^+$ moiety. The measured lifetime was 0.558 μs. The emission quantum yield ϕ was determined using triangular quartz cuvettes, as $(7 \pm 1) \times 10^{-3}$, based on the $[Ru(bipy)_3]^{2+}$ complex as reference, for which ϕ = 0.042 (λ_{exc} = 436 nm) [19]. The lack of emission from the $[Ru(bipy)_2Cl(bpz)]^+$ moiety is consistent with the fact that $[Ru(bipy)_2Cl(pz)]^{2+}$ and related $[Ru(bipy)_2XY]$ species are not good emitters at room temperature [1]. This type of behavior has been ascribed to efficient mechanisms of deactivation of the ^{3}MLCT excited state, associated with the existence of low energy ligand field states [1,20].

According to the literature [21] the MLCT excited states of ruthenium^{II}-polypyridines exhibit radical ion properties, with the unpaired electron localized on a single bipyridine group. A similar model involving electronic excitation localized on a bipyrazine ligand can be considered in our case, and according to the MO calculations (Tables 1 and 2) the excitation process would correspond to

$$[(bpz)Ru_c^{II}(bpz)Ru_p^{II}] + h\nu \rightarrow [(bpz^-)Ru_c^{III}(bpz)Ru_p^{II}]^*$$

The emission process can be represented as

$$[(bpz^-)Ru_c^{III}(bpz)Ru_p^{II}]^* \rightarrow [(bpz)Ru_c^{II}(bpz)Ru_p^{II}] + h\nu'$$

The excited state redox potentials can be estimated from the equations

$$E_{D^+/D^*} = E^0_{D^+/D} - E^{0-0} \quad (1)$$

$$E_{D^*/D^-} = E^0_{D/D^-} + E^{0-0} \quad (2)$$

where D refers to the redox/photophysically active center, $E^0_{D^+/D}$ represents the oxidation potential of the metal center (2.08 V), E^0_{D/D^-} represents the reduction potential of the bpz ligand (−0.37), and E^{0-0} is the 0–0 electronic energy. Usually, E^{0-0} has been estimated from the energy of the emission band, corresponding to 2.17 eV for the binuclear complex. In this case, the redox potentials associated with the excited state can be estimated from Eqs. (1) and (2) as $E_{D^+/D^*} = -0.09$ V and $E_{D^*/D^-} = 1.80$ V versus SHE. In fact, this is only an approximation, since as Lever and Dodsworth have pointed out [22], the evaluation of E^{0-0} from the emission energy should also include the changes in the solvent reorganization energy, χ_o. Alternatively, E^{0-0} could also be evaluated from $\Delta E = E^0_{D^+/D} - E^0_{D/D^-}$ after correcting for χ_o and the electronic term D^T, usually close to 0.48 eV for ruthenium^{II} complexes.

The excited state can decay via radiative and nonradiative pathways. The emission quantum yield ϕ_{em} (0.007, at 298 K) is related to the radiative constant k_r by [23,24]

$$\phi_{em} = \eta_{isc} k_r \tau_{exc} \quad (3)$$

where η_{isc} is the intersystem crossing efficiency and τ_{exc} the excited state life time (0.558 μs, 298 K). In the case of ruthenium polypyridines, η_{isc} is usually considered [25] very close to 1; therefore, k_r can be calculated from Eq. (3) and from the emission quantum yield, as $1.3 \times 10^4\,s^{-1}$.

On the other hand, the excited state lifetime can be expressed as (4)

$$\tau_{exc}^{-1} = k_r + k_{nr} + k_{et} \quad (4)$$

The k_{et} term represents the contribution of internal electron or energy transfer processes to the decay of the excited state. This term can be estimated from the difference of the reciprocal excited state lifetimes, τ_{exc} (0.558 μs) of the bimetallic complex and of a suitable reference complex, such as $[Ru(bpz)_3]^{2+}$, measured under the same experimental conditions ($\tau_o = 0.694$ μs, this work), (Eq. (5)).

$$k_{et} = \tau_{exc}^{-1} - \tau_o^{-1} = 3.5 \times 10^5\ s^{-1} \quad (5)$$

In this way, the nonradiative decay constant k_{nr} can be calculated from Eq. (4) as $1.4 \times 10^6\ s^{-1}$.

A possible electron transfer mechanism, in the excited state, can be represented by (6)

$$[(bpz^-)Ru_c^{III}(bpz)Ru_p^{II}]^* \rightarrow [(bpz^-)Ru_c^{II}(bpz)Ru_p^{III}] \quad (6)$$

In this case, the free energy associated with the oxidative process is given by [24,26–29]

$$\Delta G = E^0_{D/D^-} + E^0_{A^+/A} - E^{0-0} \approx 1.14 + 0.37 - 2.17 = -0.66\ eV$$

where $D = Ru_p^{II}$ and $A = Ru_c(bpz)$.

In the case of an energy transfer process, [30] the free energy associated can be estimated from the differences in the optical energies for the related $[Ru(bpz)_3]^{2+}$ (A) and $[Ru(bipy)_2(pz)Cl]^+$ (D) complexes, i.e.

$$\Delta G = E^{0-0}_{A^*/A} - E^{0-0}_{D^*/D} \approx= -0.29\ eV \quad (7)$$

Therefore, electron transfer in the excited bimetallic complex is expected to predominate over energy transfer. The electron transfer mechanism seems to be reflected in the contrasting emission lifetimes observed at room temperature (0.558 μs) and at 77 K (9.4 μs). In general, electron transfer is less effective in solid glassy solvents at 77 K, because of the outer-sphere reorganization requirements involved [25,28,31–33], thus, increasing the luminescence lifetimes.

The time resolved, differential absorption spectrum of the transient species is shown in Fig. 3, in comparison with the absorption spectrum of the starting complex. The transient absorption signal around 430 nm reflects the bleaching of the MLCT band in the starting $[Ru(bpz)_3]^{2+}$ chromophore, while the rise of the absorption bands at 380 and 750 nm is consistent with the formation of the bpz^- radical species, as expected for the excited bimetallic complex, $[(bpz^-)Ru_c^{III}(bpz^-)Ru_p^{II}]^*$. An interesting point is the observed bleaching of the absorption around 600 nm. This absorption coincides with the MLCT bands in the $[Ru^{II}(bipy)_2(bpz)Cl]^+$ moiety, and the observed changes can only be interpreted in terms of the occurrence of an intramolecular electron transfer process, generating the $[Ru_c^{II}$-(bpz^-)-$Ru_p^{III}]$ species, as represented by Eq. (6), in parallel with the radiative and non-radiative decay processes.

The decay of the $[(bpz^-)Ru_c^{II}$-(bpz)-$Ru_p^{III}]$ transient species has been measured by means of flash-photolysis, proceeding according to a first order process with $k = 1.3 \times 10^6\ s^{-1}$, regenerating the starting $[(bpz)Ru_c^{II}$-(bpz)-$Ru_p^{II}]$ complex. The overall process can be visualized in Fig. 4.

3.2. Photophysical behavior of the diad $[Ru^{II}(bpz)_3Fe^{II}(CN)_5]^-$

The bimetallic complex $[Ru^{II}(bpz)_3Fe^{II}(CN)_5]^-$ can be readily generated in aqueous solution, by the direct reaction

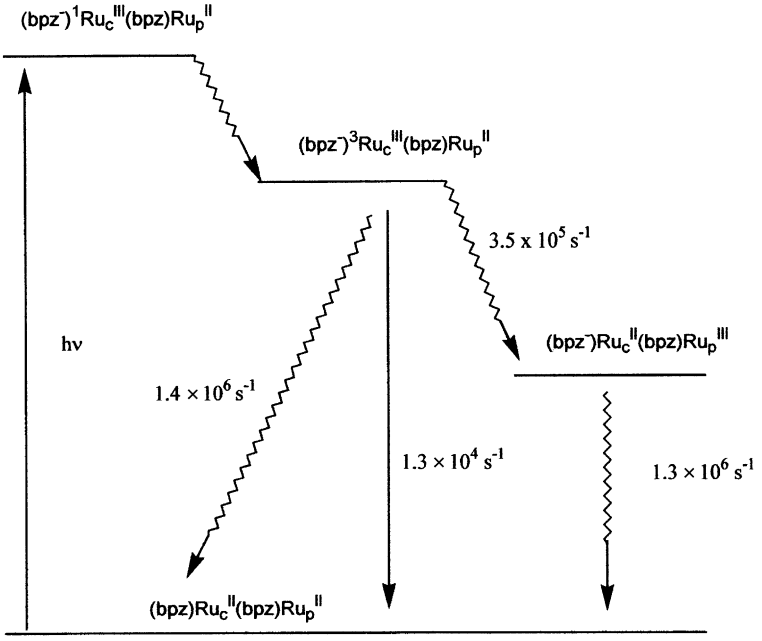

Fig. 4. Schematic representation of the deactivation pathways for the $[Ru^{II}(bpz)_3Ru^{II}(bipy)_2Cl]^{3+}$ excited species.

of stoichiometric amounts of the $[Ru^{II}(bpz)_3]^{2+}$ and $[Fe(CN)_5NH_3]^{3-}$ complexes, as previously reported by Toma and Lever [6]. The system exhibits an equilibrium constant of $7.6 \times 10^7\,M^{-1}$, reflecting the high affinity of the pentacyanoferrate^{II} ions for aromatic *N*-heterocyclic ligands [6,34,35] as well as, the favorable electrostatic factor involved in the association of the +2 and −3 charges. The binding of the pentacyanoferrate^{II} complex leads to the rise of a characteristic absorption band at 660 nm ($\varepsilon = 8.4 \times 10^3\,M^{-1}\,cm^{-1}$) ascribed to a Fe^{II}-to-(bpz) $d_{\pi} \rightarrow p_{\pi^*}$ charge-transfer transition. This process is accompanied by the decay of the emission band at 600 nm associated with the $[Ru(bpz)_3]^{2+}$ center.

The electrochemistry of this complex has already been reported in the literature [6]. exhibiting a reversible wave at $E_{1/2} = 0.70$ V versus SHE, ascribed to the $Fe^{III/II}$ redox couple.

The quantum yield for the emission in the $[Ru^{II}(bpz)_3Fe(CN)_5]^-$ complex was rather small, around 0.003, precluding accurate luminescence lifetime measurements at room temperature. The time resolved absorption spectrum of the intermediate species was similar to that observed for the $[Ru^{II}(bpz)_3Ru^{II}(bpy)_2Cl]^{3+}$ system (Fig. 5) exhibiting the decay of $[Ru(bpz)_3]^{2+}$ MLCT band at 430 nm, and the rise of the absorption band at 380 and 750 nm ascribed to the bpz^- ligand. The growth of the radical ion absorption band is partially compensated by the bleaching of the Fe^{II}-to-bpz charge-transfer band at 660 nm. Analogously to the $[Ru^{II}(bpz)_3Ru^{II}(bpy)_2Cl]^{3+}$ case, the observed changes are consistent with the occurrence of an intramolecular electron transfer process in the $[Ru^{III}(bpz^-)Fe^{II}]^*$ excited state, competing with the radiative and nonradiative decay, leading to the $[Ru^{II}(bpz^-)Fe^{III}]$ intermediate species. The decay of this species, generating the starting complexes, was monitored by flash-photolysis, leading to a first-order rate constant of $4.7 \times 10^5\,s^{-1}$.

From the experimental results in both cases, it is surprising that the charge-recombination involving the bpz^- radical is relatively slow. According to the previous studies [22] on ruthenium–polypyridine complexes, and to the theoretical calculations carried in this work, the radical ion character in this type of system is not delocalized over all the *N*-heterocyclic ligands, but it is preferentially localized on a specific ligand. In our case, it should be noted that the bridging bpz ligand is involved in π-backbonding interactions with the $[Ru^{II}(bipy)_2Cl]^+$ or $[Fe^{II}(CN)_5]^{3-}$ moieties. If π-backbonding is strong enough, as suggested by the $Ru^{II}_p \rightarrow$ bpz and $Fe^{II} \rightarrow$ bpz charge-transfer transitions at 570 and 660 nm, respectively, the empty π^* levels of the bridging bpz ligand would be shifted to higher energies, concomitant with the stabilization of the occupied Ru^{II}_p levels. This expectation seems to be theoretically supported by the ZINDO/S calculations and from the energies of the electronic transitions from Ru^{II}_c to the bridging (410 nm) and non-bridging (440 nm) π-levels (Table 2). As a consequence, the non-bridging bpz ligands can be preferentially involved in the formation of the radical ion species. In addition, since such non-bridging ligands are relatively distant from the two metal centers, there will be a decrease in the electron transfer rates, thus, explaining the results obtained in this work.

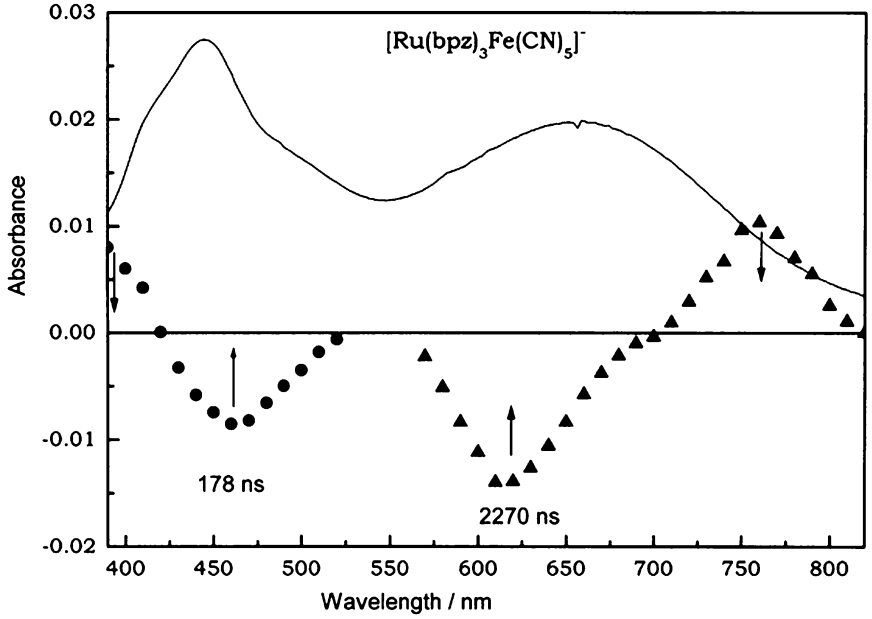

Fig. 5. Absorption profile (top, ×0.1) of the $[Ru^{II}(bpz)_3Fe(CN)_5]^-$ complex (19 μM), showing the $[Ru(bpz)_3]^{2+}$ and $[Fe(CN)_5bpz]^{3-}$ MLCT bands at 440 and 650 nm, and time resolved differential spectra (bottom) recorded at 178 and 2270 ns after laser pulse excitation.

3.3. Photophysical behavior of the triad $[(CN)_5Fe^{III}(bpz)Ru^{II}(bpz)_2Ru^{II}(bipy)_2Cl]^+$

The precursor trinuclear complex $[(CN)_5Fe^{II}(bpz)Ru^{II}(bpz)_2Ru^{II}(bipy)_2Cl]^+$ was generated in aqueous solution by reacting stoichiometric amounts of the $[Ru^{II}(bpz)_3Ru(bipy)_2Cl]^+$ and $[Fe(CN)_5NH_3]^{3-}$ complexes. In this system, two distinct bridging bipyrazine ligands are probably involved, considering the statistical factor and the expected steric hindrance effect associated with the coordination of two metal complexes to the same bipyrazine ligand. The electronic spectrum of this complex (Fig. 5) exhibits a rather broad feature covering practically all the visible region; however, the three major components associated with the characteristic MLCT bands in the $[Ru(bpz)_3]^{2+}$, $[Ru(bipy)_2(bpz)Cl]^+$ and $[Fe(CN)_5(bpz)]^{3-}$ moieties can be seen at 430, 590 and 700 nm, respectively. The three distinct moieties exhibit rather contrasting E^0 values, i.e. 2.08, 1.14 and 0.70 V, respectively. In this way, one can carry out a selective oxidation of the $[Fe(CN)_5(bpz)]^{3-}$ group, by performing a spectrophotometric titration with an aqueous chlorine solution. The oxidation of the $[Fe(CN)_5(bpz)]^{3-}$ moiety leads to the decay of the absorption band at 700 nm, so that the absorption spectrum of the mixed valence triad $[(CN)_5Fe^{III}(bpz)Ru^{II}(bpz)_2Ru^{II}(bipy)_2Cl]^-$ becomes very similar to that for the bimetallic $[Ru^{II}(bpz)_3Ru^{II}(bipy)_2Cl]^+$ complex, as one can see in Figs. 3 and 6.

As expected, the mixed valence triad did not exhibit detectable luminescence properties. However, rather interesting time resolved, differential absorption profiles have been obtained from flash photolysis experiments, as illustrated in Fig. 6.

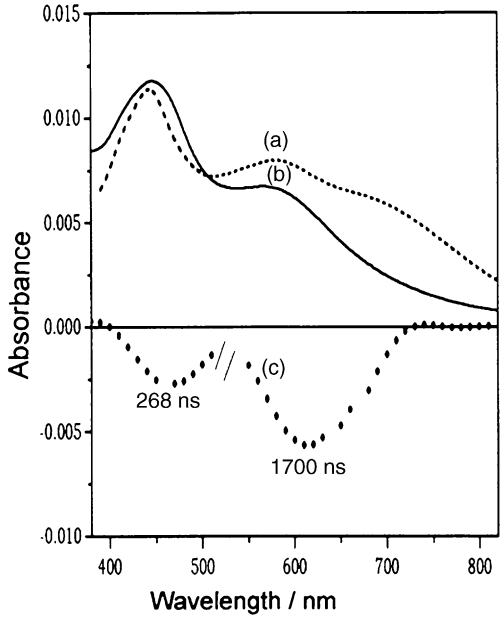

Fig. 6. Electronic absorption profile (×0.02) of the $[(CN)_5Fe^{II}(bpz)Ru^{II}(bpz)_2Ru^{II}(bipy)_2Cl]^-$ complex (33 μM) in aqueous solution (a) before chlorine oxidation of the Fe^{II} moiety, showing the $[Fe^{II}(CN)_5(bpz)]^{3-}$ MLCT band at 700 nm; (b) after the oxidation, generating the $Fe^{III}(bpz)Ru^{II}(bpz)Ru^{II}$ triad absorbing at 440 nm {MLCT $Ru(bpz)_3{}^{2+}$} and 590 nm {MLCT $Ru(bipy)_2(bpz)Cl^+$} and (c) time resolved differential spectra recorded at 258 and 1700 ns after laser pulse excitation.

Initially, in a nanosecond time scale, there is a bleaching of the absorption at 440 nm, associated with the $[Ru^{II}(bpz)_3]^{2+}$ chromophore in the trinuclear complex, generating the $[(CN)_5Fe^{III}(bpz)Ru^{III}(bpz^-)(bpz)Ru^{II}(bipy)_2Cl]^-$ excited state, as shown in the sequence (step a).

Excitation:

$$[(CN)_5Fe^{III}(bpz)_2Ru^{II}(bpz)Ru^{II}(bpy)_2Cl] \xrightarrow{h\nu} [(CN)_5Fe^{III}(bpz^-)_2Ru^{III}(bpz)Ru^{II}(bpy)_2Cl]^*$$

(a) Excited state electron transfer:

The excited state decays according to a first-order process, with $k = 7.4 \times 10^7\ s^{-1}$, regenerating the absorption band at 440 nm. This process is accompanied by the bleaching of the absorption band at 630 nm associated with the $[Ru(bipy)_2Cl]^+$ chromophore (step b). It should be noted that this absorption band is rather broad, extending above 700 nm. The narrow transient absorption profile indicates the compensation by another parallel process (step c), contributing for an increase of absorbance at 700 nm. Both processes, represented by (b) and (c) are thermodynamically favored, and can account for the excited state electron transfer processes.

$$[(CN)_5Fe^{III}(bpz^-)_2Ru^{III}(bpz)Ru^{II}(bpy)_2Cl]^* \xrightarrow{k_b} [(CN)_5Fe^{III}(bpz^-)_2Ru^{II}(bpz)Ru^{III}(bpy)_2Cl]$$

(b) $\Delta E \approx (E_{D^*/D} - E_{Ru(p)^{III/II}}) = 1.80 - 1.14 = 0.66\ V$

$$[(CN)_5Fe^{III}(bpz^-)_2Ru^{III}(bpz)Ru^{II}(bpy)_2Cl]^* \xrightarrow{k_c} [(CN)_5Fe^{II}(bpz)_2\ Ru^{III}(bpz)Ru^{II}(bpy)_2Cl]$$

(c) $\Delta E \approx (E_{Fe^{III/II}} - E_{D^+/D^*}) = 0.70 + 0.09 = 0.79\ V$

These processes should be followed by another thermodynamically favored electron transfer step (d and e), leading to long distance charge-separation.

Charge-separation:

$$[(CN)_5Fe^{III}(bpz^-)_2Ru^{II}(bpz)Ru^{III}(bpy)_2Cl] \xrightarrow{k_d} [(CN)_5Fe^{II}(bpz)_2Ru^{II}(bpz)Ru^{III}(bpy)_2Cl]$$

(d) $\Delta E \approx (E_{Fe^{III/II}} - E^0_{bpz^-}) = 0.70 + 0.37 = 1.07\ V$

$$[(CN)_5Fe^{II}(bpz)_2Ru^{III}(bpz)Ru^{II}(bpy)_2Cl] \xrightarrow{k_e} [(CN)_5Fe^{II}(bpz)_2Ru^{II}(bpz)Ru^{III}(bpy)_2Cl]$$

(e) $\Delta E \approx (E_{Ru(c)^{III/II}} - E_{Ru(p)^{III/II}}) = 2.08 - 1.14 = 0.94\ V$

The regeneration of the starting complex, via charge-recombination is relatively slow, proceeding with a first-order rate constant $k = 1.7 \times 10^6\,s^{-1}$(step f).

Charge-recombination:

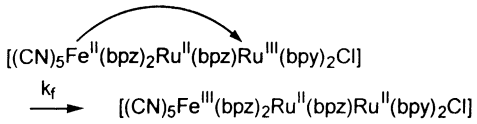

(f) $\Delta E \approx (E_{Ru(p)^{III/II}} - E_{Fe^{III/II}}) = 1.14 - 0.70 = 0.44\,V$

Thermodynamically, charge-separation seems the most plausible step involving the intermediates generated from the excited state, as indicated in steps b–e. Indeed, such intramolecular electron transfer reactions are thermodynamically favored by more than 660 mV. After this step, the charge-recombination reaction (f) should take place, but it is expected to be slower, because of the smaller driving force (440 mV), as well as of the large tunneling distance involved.

4. Conclusion

The excitation at 440 nm of the $[Ru^{II}(bpz)_3Ru^{II}(bipy)_2Cl]^{3+}$ complex leads to a ^{1}MLCT state which undergo efficient intersystem crossing to the corresponding ^{3}MLCT state, $[Ru^{III}(bpz^-)_3Ru^{II}(bipy)_2Cl]^{3+}$. The conversion to the inverted mixed valence state, $[Ru^{II}(bpz^-)_3Ru^{III}(bipy)_2Cl]^{3+}$, proceeds via electron transfer mechanisms, competing with the radiative and nonradiative decay of the ^{3}MLCT state. A similar behavior was observed for the $[Ru^{II}(bpz)_3Fe^{II}(CN)_5]^-$ complex. In the case of the $[(CN)_5Fe^{III}(bpz)Ru^{II}(bpz)_2Ru^{II}(bipy)_2Cl]^+$ triad, the excited state centered on the $[Ru(bpz)_3]^{2+}$ moiety can undergo intramolecular electron transfer reactions with the peripheral Ru^{II} and Fe^{III} groups, leading to the inverted mixed valence complex, $[(CN)_5Fe^{II}(bpz)Ru^{II}(bpz)_2Ru^{III}(bipy)_2Cl]^-$, displaying charge-separation effects.

Acknowledgements

We gratefully acknowledge the financial support from the Brazilian Agencies FAPESP and CNPq.

References

[1] V. Balzani, F. Scandola, Supramolecular Photochemistry, Harwood, West Sussex, 1991.
[2] B. Schlicke, P. Belser, L. De Cola, E. Sabbioni, V. Balzani, J. Am. Chem. Soc. 121 (1999) 4207.
[3] P. Belser, S. Bernhard, C. Blum, A. Beyeler, L. De Cola, V. Balzani, Coord. Chem. Rev. 190 (1999) 155.
[4] V. Balzani, A. Juris, Coord. Chem. Rev. 211 (2001) 97.
[5] F. Barigelletti, L. Flamigni, M. Guardigli, A. Juris, M. Beley, S. Chodorowski-Kimmes, J.-P. Collin, J.-P. Sauvage, Inorg. Chem. 35 (1996) 136.
[6] H.E. Toma, A.B.P. Lever, Inorg. Chem. 25 (1986) 176.
[7] H.E. Toma, P.A. Alburn, E.S. Dodsworth, M.N. Golovin, A.B.P Lever, Inorg. Chem. 26 (1987) 4257.
[8] H.E. Toma, P.S. Santos, A.B.P. Lever, Inorg. Chem. 27 (1988) 3850.
[9] H.E. Toma, R.L. Sernaglia, Talanta 40 (1993) 515.
[10] R.J. Crutchley, A.B.P. Lever, J. Am. Chem. Soc. 102 (1980) 7128.
[11] R.J. Crutchley, A.B.P. Lever, Inorg. Chem. 21 (1982) 2276.
[12] R.J. Crutchley, N. Kress, A.B.P. Lever, J. Am. Chem. Soc. 105 (1983) 1170.
[13] B.P. Sullivan, D.J. Salmon, T.J. Meyer, Inorg. Chem. 17 (1978) 3334.
[14] H.E. Toma, J.M. Malin, Inorg. Chem. 12 (1973) 1039.
[15] F.N. Rein, R.C. Rocha, H.E. Toma, J. Coord. Chem. 53 (2001) 99.
[16] M. Franco, K. Araki, R.C. Rocha, H.E. Toma, J. Sol. Chem. 29 (2000) 667.
[17] H.E. Toma, R.M. Serrasqueiro, R.C. Rocha, G.J.F. Demets, H. Winnischofer, K. Araki, P.E.A. Ribeiro, C.L. Donnici, J. Photochem. Photobiol. A 135 (2000) 185.
[18] V.R.L. Constantino, H.E. Toma, L.F.C. de Oliveira, F.N. Rein, R.C. Rocha, D.D. Silva, J. Chem. Soc., Dalton Trans. (1999) 173.
[19] J. Van Houten, R.J. Watts, J. Am. Chem. Soc. 97 (1975) 3843.
[20] C. Berg-Brennan, P. Subramanian, M. Absi, C. Stern, J.T. Hupp, Inorg. Chem. 35 (1996) 3719.
[21] M.K. De Armond, M.L. Myrick, Acc. Chem. Res. 22 (1989) 364.
[22] A.B.P. Lever, E.S. Dodsworth, in: E.I. Solomon, A.B.P Lever (Eds.), Inorganic Electronic Spectroscopy, Vol. II: Applications and Case Studies, Wiley, New York, 1999, p. 227.
[23] K.R. Barqawi, A. Llobet, T.J. Meyer, J. Am. Chem. Soc. 110 (1988) 7751.
[24] S. Van Wallendael, M.W. Perkovic, D.P. Rillema, Inorg. Chim. Acta 213 (1993) 253.
[25] L. De Cola, P. Belser, Coord. Chem. Rev. 177 (1998) 301.
[26] F. Barigelletti, L. De Cola, A. Juris, Gazz. Chim. Ital. 120 (1990) 545.
[27] L. Hammarström, J. Alsins, A. Börje, T. Norrby, L. Zhang, B. Akemark, J. Photochem. Photobiol. A 102 (1997) 139.
[28] R. Bergonzi, L. Fabbrizzi, M. Licchelli, C. Mangano, Coord. Chem. Rev. 170 (1998) 31.
[29] J. Van Houten, R.J. Watts, J. Am. Chem. Soc. 97 (1975) 3843.
[30] K. Kalyanasundaram, Photochemistry of Polypyridine and Porphyrin Complexes, Academic Press, New York, 1992.
[31] M.T. Indelli, F. Scandola, J.P. Collin, J.P. Sauvage, Inorg. Chem. 35 (1996) 303.
[32] J.D. Lee, L.M. Vrana, E.R. Bullock, K.J. Brewer, Inorg. Chem. 37 (1998) 3575.
[33] M.T. Indelli, C.A. Bignozzi, A. Harriman, R.J. Schnoover, F. Scandola, J. Am. Chem. Soc. 116 (1994) 3768.
[34] H.E. Toma, C. Creutz, Inorg. Chem. 16 (1977) 550.
[35] H.E. Toma, A.A. Batista, H.B. Gray, J. Am. Chem. Soc. 104 (1982) 7509.